

## Effect of $p-n$ junction parameters on the optimization of contact design in photovoltaic converters of laser radiation

© M.A. Mintairov, V.V. Evstropov, A.D. Malevskaya, S.A. Mintairov, M.Z. Shvartz, N.A. Kalyuzhnyi

Ioffe Institute, St. Petersburg, Russia  
E-mail: mamint@scell.ioffe.ru

Received July 23, 2025

Revised October 8, 2025

Accepted October 9, 2025

It is demonstrated that the magnitude of saturation currents of  $p-n$  junctions in photovoltaic converters of laser radiation has a critical influence on the processes of current spreading between finger contacts and, consequently, largely determines the choice of the optimum design of the front contact grid. The optimum designs of contact grids for photovoltaic converters of laser radiation with different band gaps  $E_g$  are calculated by varying the value of spreading sheet resistance  $R_{SHEET}$  and width  $W_m$  of finger contacts.

**Keywords:** photovoltaic converters, solar cells, spreading resistance, contact resistance.

DOI: 10.61011/TPL.2026.02.63040.20452

It is known that thorough optimization of the front contact grid of photovoltaic converter (PVC) chips designed to absorb high power densities of incident radiation is needed to reach high levels of efficiency of their operation [1–4]. The solution to this optimization problem comes down to finding a compromise between the values of resistive and optical losses [2,4,5]. Specifically, an increase in density of a finger contact grid leads to a reduction in resistive losses, but increases optical losses due to shading of the absorbing PVC surface. The issues of optimum design of contact grids and the main approaches to their optimization are well-studied [2,6–9]. These approaches rely on calculations of distributed equivalent circuits with the processes of current spreading between finger contacts taken into account. The key factor determining the calculation results is the value of spreading sheet resistance ( $R_{SHEET}$ ). This parameter in modern concentrator solar cells converting high levels of incident radiation power assumes values on the order of  $550 \Omega \cdot \text{sq}^{-1}$  and may be reduced to  $250 \Omega \cdot \text{sq}^{-1}$  [1]. The impossibility of significant thickening of surface layers of the emitter and the wide-gap „window“ over which the current spreads imposes a limit on further reduction of  $R_{SHEET}$  in solar cells. Specifically, since the solar spectrum has a wide range of wavelengths, thickening of the wide-band „window“ will lead to an increase in absorption of a fraction of incident radiation in it. The design of PVCs of laser radiation allows [10–12] for the introduction of an additional near-surface spreading layer (Fig. 1) with a thickness of several micrometers that is made of a semiconductor material transparent to incident radiation. This layer makes it possible to reduce  $R_{SHEET}$  to  $15\text{--}50 \Omega \cdot \text{sq}^{-1}$  [2,13] or even lower levels. A number of models and methods for calculating the main parameters of PVCs as functions of  $R_{SHEET}$  are available [4,7,8,14–16]. Most studies in this field are focused on the analysis of calculation results and optimization of contacts of PVCs with varying resistive

parameters (i.e., parameters of the so-called connection PVC part [15]: metal contacts and all semiconductor layers located outside the photoactive  $p-n$  junction; see Fig. 1). The resistance of the connection part may be divided into lateral resistance ( $R_L$ ), which characterizes the resistance along the  $p-n$  junction, and vertical resistance ( $R_V$ ), which characterizes the resistance in the direction perpendicular to the  $p-n$  junction. The metal contact resistance, the metal–semiconductor contact resistance, and the resistance of the substrate and epitaxial layers are included into  $R_V$ , while  $R_L$  includes the lateral resistance of emitter layers, the wide-gap window, and spreading of current between finger contacts (Fig. 1). No studies investigating the influence of parameters of  $p-n$  junctions (parameters of the generator PVC part, which includes the photoactive  $p-n$  junction; see Fig. 1) on the result of optimization of PVC contact grids have been published to date, while the distributed nature of the equivalent circuit used to characterize current spreading indicates clearly that the calculation result is affected by a change in any circuit parameter (including the parameters of  $p-n$  junctions). In other words, if two PVC samples are manufactured with the same connection part and  $p-n$  junctions made from different materials, the magnitudes of voltage drop across the same resistive elements of the PVC structure will differ due to the distributed nature of current spreading. Therefore, devices with different  $p-n$  junctions will have distinct optimum designs of the PVC contact grid. This fact has not yet been discussed in literature.

In the present study, we examine the influence of the  $p-n$  junction parameters on the choice of contact grid design. The main parameters of the  $p-n$  junction of a PVC are its saturation currents ( $J_{01}$  and  $J_{02}$  are the currents with ideality factors  $A = 1$  and  $2$ , respectively) and the spectral response ( $SR$ ) magnitude. Spreading sheet resistance  $R_{SHEET}$ , finger contact spacing  $W$ , and finger contact width  $W_m$  were chosen as the main parameters specifying the design of contacts.

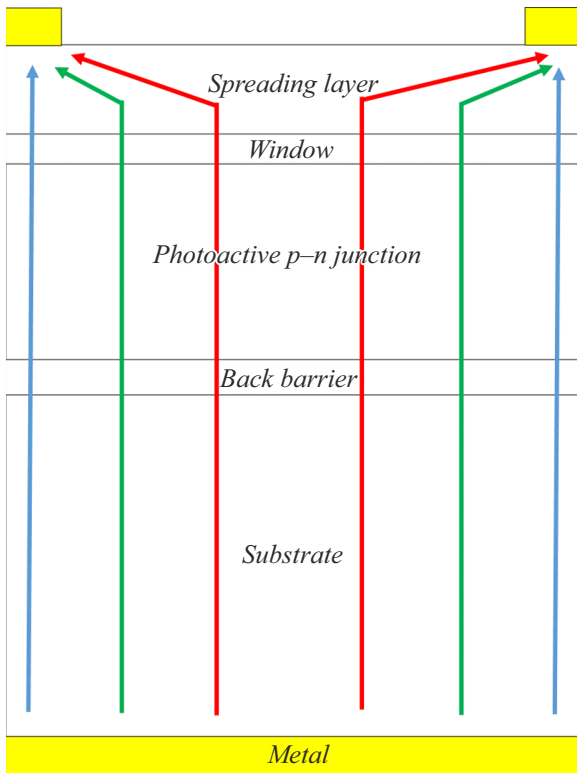


**Figure 1.** Layer-by-layer diagram of a laser radiation PVC with a schematic illustration of current spreading under the finger contacts.

Calculations were carried out using the tube model of current spreading that was developed earlier in [15]. The model calculates PVC current–voltage curves (CVCs) as functions of photogenerated current  $J_g$ , saturation currents  $J_{01}$  and  $J_{02}$ , and two resistive parameters  $R_L$  and  $R_V$ . According to the model,

$$R_L = R_{SHEET} \left( \frac{W}{2} \right)^2, \quad (1)$$

which means that it may be calculated based on the main specified parameters  $W$  and  $R_{SHEET}$ . The vertical resistance may be neglected, since it is several orders of magnitude lower than the spreading resistance [15]. The saturation currents were calculated using the current invariant model [17], which allowed us to determine the values of  $J_{01}$  and  $J_{02}$  as functions of band gap  $E_g$  of the  $p-n$  junction. The PVC photocurrent is normally determined from the quantum efficiency ( $QE$ ) spectrum of the photoresponse, which is a dimensionless quantity that characterizes the ratio of the number of electron–hole pairs separated by the photoactive  $p-n$  junction to the number of photons incident on the PVC surface. In the case of PVCs operating with laser radiation, spectral response  $SR$ , which is a formalization of quantum efficiency in  $A/W$  units, is more convenient. The  $SR$  spectrum is derived from the  $QE$

one in the following way:

$$SR(\lambda) = \frac{q}{hc} \lambda \cdot QE(\lambda), \quad (2)$$

where  $\lambda$  is the wavelength,  $q$  is the electron charge,  $h$  is the Planck constant, and  $c$  is the speed of light.

Assuming that the laser radiation photon energy is equal to  $E_g$  of the photoactive  $p-n$  junction material and  $QE = 1$ , we obtain an expression for the spectral response for the open surface:

$$SR_0 = \frac{q}{E_g}. \quad (3)$$

The surface shading coefficient ( $W_m/W$ ) was then calculated, and the spectral PVC response was determined after that:

$$SR = SR_0 \frac{W_m}{W}. \quad (4)$$

The photogenerated current was calculated in the following manner:

$$J_g = SR \cdot P_{inc}, \quad (5)$$

where  $P_{inc}$  is the specified incident radiation power.

Thus, one may calculate the PVC CVC specified by the following four parameters at any incident radiation power  $P_{inc}$ :  $W$ ,  $W_m$ ,  $E_g$ , and  $R_{SHEET}$ . The calculated CVC provides an opportunity to determine optimum load power  $P_m$  and, consequently, the device efficiency

$$Eff = P_m/P_{inc}. \quad (6)$$

This procedure was used to determine the dependences of optimum finger contact spacing on the band gap of the  $p-n$  junction for different combinations of  $W_m$  (this parameter was varied from 5 to 15  $\mu\text{m}$ ) and  $R_{SHEET}$  (from 10 to 50  $\Omega \cdot \text{sq}^{-1}$ ). In these calculations, gold was assumed to be the material of finger contacts, and their height was 2  $\mu\text{m}$ .

The calculation results are shown in Fig. 2. The obtained dependences suggests that the band gap exerts a critical influence on the choice of the optimum design of the front PVC contact grid regardless of the thickness of finger contacts. It is also evident that as the spreading sheet resistance increases, its influence on the optimum finger contact spacing grows weaker, and it becomes difficult to choose the optimum design based on this parameter.

One important result of calculations was that an increase in  $E_g$  of the  $p-n$  junction makes it possible to increase the distance between finger contacts, which is equivalent to reducing the spreading resistance. This is attributable to the fact that an increase in  $E_g$  of the  $p-n$  junction translates into a greater voltage drop across the diodes in the distributed equivalent circuit; i.e., under the same illumination conditions, the voltage drop across the generator PVC part is greater, which leads to a more uniform flow of current across the PVC structure and a suppression of the voltage drop across the connection PVC part. Thus, as  $E_g$  of the  $p-n$  junction increases, the series resistance

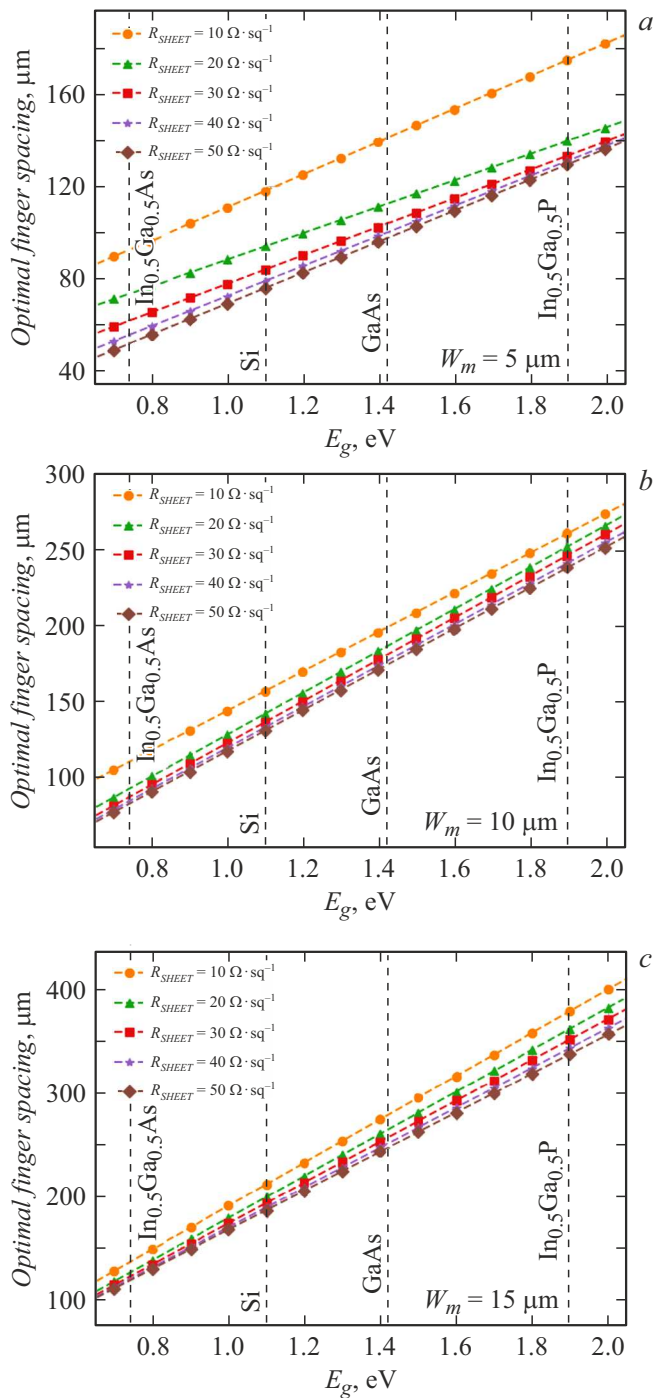


**Figure 2.** Dependences of the optimum finger contact spacing on the band gap of the  $p-n$  junction at different values of spreading sheet resistance  $R_{SHEET}$ . Three calculations were performed with different contact widths:  $W_m = 5$  (a), 10 (b), and 15 μm (c).

becomes less significant in comparison with the diode resistance. The CVC of the connection PVC part changes due to this variation of current distribution. In the region of currents close to the optimum load current, the spreading resistance decreases with an increase in  $E_g$  of the  $p-n$  junction.

Taken into account, this effect may exert a significant influence on the PVC efficiency, since an increase in  $E_g$  of the  $p-n$  junction from 1 to 1.6 eV provides an opportunity to reduce the shading of the front PVC surface by the contact grid by a factor of more than 2: from 8–9 to 3–4% (Fig. 1).

It is also important to note that the resistance of finger contacts affects significantly the PVC CVC, since an increase in their width allows for a potentially significant increase in distance between them. While the optimum distance for fingers 5 μm in width varies, depending on the sheet resistance, from 80 to 150 μm, the same distance for fingers with a width of 15 μm varies from 180 to 320 μm. However, the shading of the front surface by these fingers remains virtually unchanged in this case.

Thus, it was demonstrated that the saturation currents of the  $p-n$  junction need to be taken into account when one calculates the optimum design parameters of the contact grid of PVCs operating in high-power laser radiation conversion regimes. The values of saturation currents may either be estimated based on the band gap of the  $p-n$  junction material (using, e.g., a current invariant) or determined experimentally by analyzing the device CVCs.

### Conflict of interest

The authors declare that they have no conflict of interest.

### References

- [1] M. Klitzke, P. Schygulla, J. Schön, O. Höhn, G. Siefer, H. Helmers, F. Dimroth, D. Lackner, *Solar RRL*, **8** (10), 2400150 (2024). DOI: 10.1002/solr.202400150
- [2] H. Helmers, E. Oliva, M. Schachtner, G. Mikolasch, L.A. Ruiz-Preciado, A. Franke, J. Bartsch, *Prog. Photovolt.: Res. Appl.*, **32** (9), 636 (2024). DOI: 10.1002/pp.3804
- [3] T.A. Gessert, X. Li, T.J. Coutts, *Solar Cells*, **30** (1-4), 459 (1991). DOI: 10.1016/0379-6787(91)90078-4
- [4] N.A. Kalyuzhnyy, A.V. Malevskaya, S.A. Mintairov, M.A. Mintairov, M.V. Nakhimovich, R.A. Salii, M.Z. Shvartz, V.M. Andreev, *Solar Energy Mater. Solar Cells*, **262**, 112551 (2023). DOI: 10.1016/j.solmat.2023.112551
- [5] A.D. Malevskaya, M.A. Mintairov, V.V. Evstropov, D.A. Malevskiy, N.A. Kalyuzhnyy, *Semiconductors*, **58** (10), 528 (2024). DOI: 10.61011/SC.2024.10.59948.6619A.
- [6] R.J. Handy, *Solid-State Electron.*, **10** (8), 765 (1967). DOI: 10.1016/0038-1101(67)90159-1
- [7] A. De Vos, *Solar Cells*, **12** (3), 311 (1984). DOI: 10.1016/0379-6787(84)90110-8
- [8] C. Algora, V. Díaz, *Prog. Photovolt.: Res. Appl.*, **8** (2), 211 (2000). DOI: 10.1002/(SICI)1099-159X(200003/04)8:2<211::AID-PIP291>3.0.CO;2-D
- [9] M. Steiner, S.P. Philipps, M. Hermle, A.W. Bett, F. Dimroth, *Prog. Photovolt.: Res. Appl.*, **19** (1), 73 (2010). DOI: 10.1002/pp.989
- [10] C. Algora, I. García, M. Delgado, R. Peña, C. Vázquez, M. Hinojosa, I. Rey-Stolle, *Joule*, **6**, 340 (2022). DOI: 10.5281/zenodo.6620474

- [11] S. Fafarda, D.P. Masson, J. Appl. Phys., **130** (16), 160901 (2021). DOI: 10.1063/5.0070860
- [12] H. Helmers, E. Lopez, O. Höhn, D. Lackner, J. Schön, M. Schauerte, M. Schachtner, F. Dimroth, A.W. Bett, Phys. Status Solidi RRL, **15** (7), 2100113 (2021). DOI: 10.1002/pssr.202100113
- [13] E. Oliva, F. Dimroth, A.W. Bett, Prog. Photovolt.: Res. Appl., **16**, 289 (2008). DOI: 10.1002/pip.811
- [14] M.N. Beattie, H. Helmers, G.P. Forcade, C.E. Valdivia, O. Höhn, K. Hinzer, IEEE J. Photovolt., **13** (1), 113 (2023). DOI: 10.1109/JPHOTOV.2022.3218938
- [15] M.A. Mintairov, V.V. Evstropov, S.A. Mintairov, N.Kh. Timoshina, M.Z. Shvarts, N.A. Kalyuzhnyy, Semiconductors, **50** (7), 970 (2016). DOI: 10.1134/S1063782616070162.
- [16] V.M. Emelyanov, N.A. Kalyuzhnyy, M.A. Mintairov, S.A. Mintairov, M.Z. Shvarts, V.M. Lantratov, in *Proc. of the 25th European Photovoltaic Solar Energy Conf. and Exhibition/5th World Conf. on Photovoltaic Energy Conversion* (Valencia, Spain, 2010), vol. 2.33, p. 406. DOI: 10.4229/25THEUPVSEC2010-1DV.2.33
- [17] M.A. Mintairov, V.V. Evstropov, S.A. Mintairov, M.V. Nakhimovich, R.A. Saliı, M.Z. Shvarts, N.A. Kalyuzhnyy, Solar Energy Mater. Solar Cells, **264**, 112619 (2024). DOI: 10.1016/j.solmat.2023.112619

*Translated by D.Safin*